

Thermochemistry, Reaction Paths, and Kinetics on the Hydroperoxy-Ethyl Radical Reaction with O₂: New Chain Branching Reactions in Hydrocarbon Oxidation

Joseph W. Bozzelli* and Chad Sheng

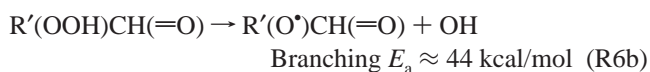
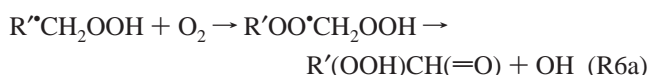
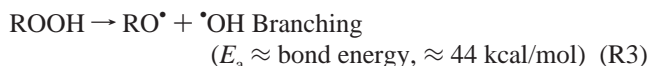
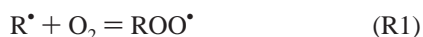
Department of Chemical Engineering, Chemistry and Environmental Science,
New Jersey Institute of Technology, Newark, New Jersey 07102

Received: September 21, 2001; In Final Form: December 14, 2001

Ab initio and density functional calculations are performed to determine thermochemical and kinetic parameters in analysis of the 2 hydroperoxy-ethyl radical association with O₂. The system serves as an initial model for O₂ association with higher molecular weight alkyl-hydroperoxide radicals and is an important component in the well-studied ethyl radical plus O₂ reaction system. The CBS-Q//B3LYP/6-31G(d,p) and G3(MP2) composite methods are utilized to calculate energies. The well depth is determined as 35 kcal/mol and transition state results show two low energy paths (barriers below the entrance channel) for reaction to new products: (i) a HO₂ molecular elimination and (ii) a hydrogen shift path. Intramolecular hydrogen transfer (five-member ring) leads to 2 hydroperoxide acetadehyde + OH, where the barrier is ca. 7 kcal/mol lower than previously estimated. The HOOCH₂CH(=O) formed here is chemically activated and a significant fraction dissociates to OH + formyl-methoxy radical, before stabilization. The barrier for hydrogen transfer is several kcal/mole lower than the corresponding reaction in a conventional hydrocarbon for this five-member ring transition state because the weak C–H bond on the hydroperoxide carbon. The second path is unimolecular HO₂ elimination leading to a vinyl hydroperoxide + HO₂. The vinyl hydroperoxide has a weak (22.5 kcal/mol) CH₂=CHO–OH bond and rapidly dissociates to formyl methyl plus OH radicals; a second low energy chain branching path in low-temperature HC oxidation. Kinetic analysis with falloff on chemical activation and unimolecular dissociation, illustrate that both low energy paths are competing. Results also show significant formation of a diradical, [•]OCH₂CH₂OO[•] + OH, an additional new path to chain branching, which results from the chemical activation reaction. The HO₂ molecular elimination plus vinyl hydroperoxide dominates the H transfer by a factor of 1.8 at low temperatures, a result of its small entropy advantage. At high temperatures, dissociation to the higher energy, but loose transition state, hydroperoxide ethyl radical + O₂ (back to reactants) is the dominant path.

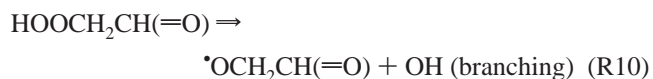
Introduction

The conventional approach to describe low-temperature ignition kinetics, especially in the negative temperature coefficient regime, considers the following reactions of peroxy species¹



R[•] is an alkyl radical, RO[•] is an alkoxy radical and Cy-R'CO is a cyclic ether. R[•]CH₂OOH is often written as QOOH; we use the R[•]CH₂OOH notation to emphasize the free radical character of this species. We write (R4) slightly differently than Walker,¹

to distinguish radical formation on the carbon bonded to peroxide versus other carbons; the radical formed is not on the peroxide carbon. If the temperature is sufficiently low that the equilibrium in (R1) is shifted to the right, the subsequent reactions of ROO[•] can lead to the chain branching needed to model ignition and cool flames (R3 and R6). However, as the temperature rises, the equilibrium in (R1) shifts to the left, reducing the ROO[•] concentration and R[•] conversion. This slows the overall oxidation rate and produces a negative temperature coefficient for conversion of alkanes. The isomerization in reaction (R4) is important because it is needed for chain branching. The alkyl radical which is formed reacts further with O₂ (R6a and R6b above exemplified for ethyl in this study).



We note that $\cdot\text{CH}_2\text{OOH}$ and $\text{RC}\cdot\text{H}_2\text{OOH}$ rapidly dissociate to $\text{CH}_2=\text{O} + \text{OH}$ (and $\text{RCH}_2=\text{O} + \text{OH}$) with no barrier; because the carbonyl bond formed is so much stronger (ca 80 kcal/mol) than the peroxide ($\text{RO}-\text{OH}$, ca. 45 kcal/mol) bond cleaved.

In this study, we use the composite CBS-Q and G3(MP2) calculations to estimate enthalpies of the adduct and transition states in the hydroperoxy-ethyl + O_2 reaction system. Two reaction paths, which have lower energies than the (entrance channel) are found: a direct elimination to HO_2 plus $\text{H}_2\text{C}=\text{CHOOH}$ and a 1,4 hydrogen shift (five-member ring) transition state structure to $(\text{HOOCH}_2\text{C}\cdot\text{HOOH})^*$, which immediately dissociates to $\text{HOOCH}_2\text{CH}(\text{=O}) + \text{OH}$. The direct HO_2 elimination is a new reaction path not previously considered in this di-peroxy system; the vinyl-hydroperoxide formed ($\text{H}_2\text{C}=\text{CHOOH}$) dissociates rapidly with an E_a of about 22.5 kcal/mol, leading to low energy chain branching channel. The hydrogen shift and direct HO_2 elimination path are found to have similar kinetics. Relative to the five-member ring H-shift in the ethyl-peroxy radical, the hydrogen shift is found to have a more important role in this hydroperoxide-peroxy system, because the peroxy oxygen is abstracting from a weak C-H bond on $\text{R}-\text{CH}_2\text{OOH}$. The H-shift path also results in some chain branching because the $\text{HOOCH}_2\text{CH}(\text{=O})$ formed is chemically activated and a fraction dissociates to $\text{OH} +$ formyl-methoxy radical, before stabilization.

A third path to chain branching is also apparent: chemical activation association of the hydroperoxy-ethyl + O_2 , which has 35 kcal/mol of energy relative to the stabilized adduct, results in a diradical $\cdot\text{OCH}_2\text{CH}_2\text{OO}\cdot + \text{OH}$ from hydroperoxide O-O bond cleavage. This is about 9 kcal/mol above entrance channel, but has a loose transition state structure.

Calculation Methods

Thermodynamic Properties. Molecular properties for reactants, adducts, transition states (TS) and products are estimated by the composite CBS-Q² and by G3(MP2)³ methods using Gaussian94.⁴ The hybrid DFT method B3LYP, with a double- ζ polarized basis set, 6-31G(d,p), is used to determine the optimized geometry for CBS-Q calculations,^{5,6} denoted as CBS-Q//B3LYP/6-31G(d,p), and MP2(full)/6-31G(d) is used for G3(MP2). The DFT calculations are spin-unrestricted Hartree-Fock. Molecular geometries are fully optimized using the Berny algorithm and redundant internal coordinates.⁴ Confirmation of TS structures is verified by checking for a single imaginary frequency and its motion, plus evaluation of the optimized TS structures. The spin contamination for all three saddle point TS's is 0.76, in the B3LYP/6-31G(d,p) calculations, in reasonably close agreement with the theoretical spin value of 0.75.

Statistical mechanics is employed to determine the vibration, external rotational and translational contributions to entropy and Cp(T). Molecular parameters required in the statistical mechanics analysis are calculated at the B3LYP/6-31G(d,p) level of theory for the optimized geometric structure of the species. Zero-point vibration energy (ZPVE), vibration frequency and thermal contributions to enthalpy from harmonic frequencies are scaled in accordance to the factors recommended by Scott and Radom.⁷ Contributions from optical isomers and unpaired electrons are included in the S^{298} calculations accordingly. The active carbon site has chiral characteristics, in addition to presence of optical isomers from the hydroperoxy group. The hydroperoxy being formed in the ring (TS) does not contribute to a second optical isomer because it is part of the chiral characteristic. Contributions of internal rotation to S^{298} and Cp(T) are incorporated based on the Pitzer-Gwinn formalism.⁸

Determination of Rate Constants. The high-pressure limit rate constants are determined by application of macrocanonical transition state theory for temperatures from 250 to 2500 K. The rate constants are fitted by a nonlinear least-squares method to the form of a modified Arrhenius rate expression, $k_{\infty,forw} = A_{\infty}T^n e^{-(E_a/RT)}$, to obtain the parameters: A_{∞} , n , and E_a . The reported rate constants are derived from the enthalpy of formation calculated at the CBS-Q//B3LYP/6-31G(d,p) level of theory and entropy and heat capacity values at B3LYP/6-31G(d,p) level of theory. The CBS-Q analysis is used, as opposed to G3(MP2), because of significantly lower spin contamination in several species. The rate constant for the $\cdot\text{CH}_2\text{CH}_2\text{OOH} + \text{O}_2 \rightleftharpoons \text{HOOCH}_2\text{CH}_2\text{OO}\cdot$ reaction is estimated based on the variational transition state theory for ethyl + O_2 .⁹ The dissociation (reverse rate constant) is based on microscopic reversibility. The rate constant for



is estimated from ΔH_{rxn} and literature values for the A factor of O-O bond cleavage in hydroperoxides.¹⁰

This overall $\cdot\text{CH}_2\text{CH}_2\text{OOH} + \text{O}_2 \rightleftharpoons \text{HOOCH}_2\text{CH}_2\text{OO}\cdot$ reaction process is complex, involving several competitive reactions of the energized and stabilized adduct: which has 4 forward paths plus a reverse reaction with a loose transition state, all at competitive energies. In addition stabilization and one higher energy isomerization with a tight transition state are present. A weak (ca 1 kcal/mol well) hydrogen bonding conformer of the adduct is also present.

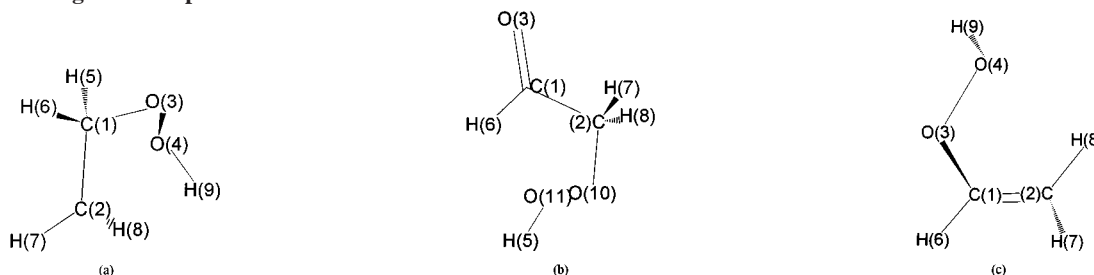
Kinetic parameters describing product formation from the bimolecular chemical activation association process and the unimolecular thermal dissociations are estimated using a multi-frequency quantum Rice-Ramsperger-Kassel (QRRK) analysis for $k(E)$ ¹¹⁻¹⁴ with the steady-state assumption on the energized adduct and master equation analysis¹⁵⁻¹⁷ for falloff. Chang et al.^{14,18} described a modified QRRK analysis that is used in this paper.

Results and Discussion

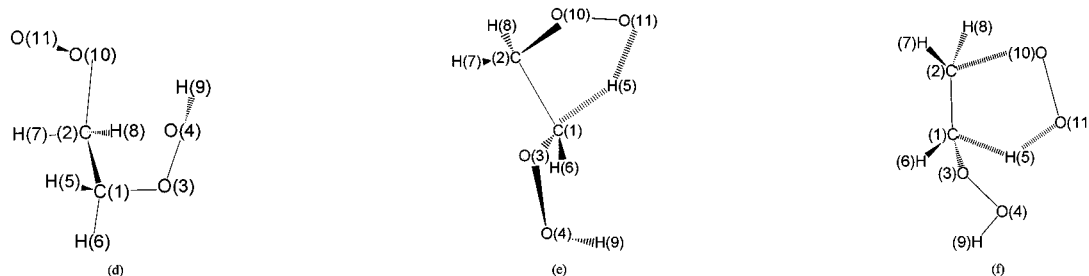
Structures. Table 1 lists the optimized structure parameters and Table 2 lists the unscaled vibrational frequencies and moments of inertia from the B3LYP/6-31G(d,p) level of theory. Figure 1 shows an overall energy diagram of the reaction paths. The lowest energy conformer, a cyclic hydrogen bonded intermediate, is 0.85 and 1.02 kcal/mol lower in energy than the more linear alkyl like structure calculated at B3LYP/6-31G(d,p) and UHF/6-31G(d), respectively.

Hydrogen Shift Isomerization (Five-Member Ring) – TS1. The TS for the hydrogen shift of $\text{HOOCH}_2\text{CH}_2\text{OO}\cdot$ to $\text{HOOCH}_2\text{CH}(\text{=O}) + \text{OH}$, via a five-member ring, (TS1) forms an unstable $\text{HOOCH}_2\text{C}\cdot\text{HOOH}$, which rapidly dissociates (elimination of OH) to form the hydroperoxy-acetaldehyde + OH product. This second reaction (after the H-shift) is similar to the instability in the hypochlorite-methyl radical, where $\cdot\text{CH}_2\text{O}-\text{Cl}$ dissociation to lower energy products $\text{CH}_2\text{O} + \text{Cl}$ exhibits no barrier.¹⁹ The structure of TS1 infers the start of the second reaction step, elimination of OH from the hydroperoxy on the β -carbon, since the C-O bond length is 1.37 Å, which is slightly shorter than the normal C-O bond length of 1.46 Å.²⁰ This suggests that TS1 continues through an unstable dihydroperoxy-ethyl radical structure, which quickly dissociates by breaking the weak (ca 45 kcal/mol) hydroperoxy bond while forming the stronger (ca 80 kcal/mol) carbonyl bond.

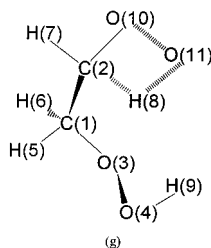
TABLE 1: Optimized Geometric Parameters for Species in the Hydroperoxy–Ethyl + O₂ Oxidation System at the B3LYP/6-31G(d,p) Level of Theory: (a) Hydroperoxy–Ethyl Radical (b) Hydroperoxy–Acetaldehyde (c) Hydroperoxy–Ethylene (d) Hydroperoxy–Ethylperoxy (e) Five-Member Ring H-Shift TS (f) Five-Member Ring Molecular Elimination TS (g) Four-Member Ring H-Shift Ipro-Carbon



*CH ₂ CH ₂ OOH				HOOCH ₂ CH(=O)				H ₂ C=CHOOH			
parameter ^d	value	parameter ^d	value	parameter ^d	value	parameter ^d	value	parameter ^d	value	parameter ^d	value
r21	1.4867	a312	113.51	r21	1.5225	a312	123.20	r21	1.3294	a612	124.20
r31	1.4338	a512	111.64	r31	1.2083	a612	114.24	r31	1.3715	a943	99.97
r51	1.1028	a612	111.78	r61	1.1126	a11102	104.30	r61	1.0873	d9431	105.50
r61	1.0964	a943	100.62	r72	1.0971	a51110	99.07	r72	1.0825	d4312	-2.24
r72	1.0839	d9431	-100.13	r82	1.0981	d111021	-68.62	r82	1.0810	d6123	179.93
r82	1.0857	d4312	70.81	r102	1.4116	d511102	145.97	r43	1.4477	d7213	-179.85
r43	1.4545	d8217	-175.59	r1110	1.4669	d82110	115.43	r94	0.9725	d8213	1.20
r94	0.9715	d3127	-138.25	r511	0.9708	d72110	-125.68	a431	110.61		
a431	107.08	d5127	107.51	a721	110.17	d31210	-193.36	a721	118.94		
a721	121.63	d6127	-13.42	a821	109.09	d61210	-15.04	a821	122.06		
a821	119.65			a1021	112.47			a312	128.85		



HOOCH ₂ CH ₂ OO*				TS1				TS2			
parameter ^d	value	parameter ^d	value	parameter ^d	value	parameter ^d	value	parameter ^d	value	parameter ^d	value
r21	1.5226	a312	112.71	r21	1.5338	a312	111.68	r21	1.3899	a312	115.06
r31	1.4205	a512	110.64	r31	1.3720	a612	117.54	r31	1.4008	a612	119.67
r51	1.0946	a612	108.66	r61	1.0923	a11102	103.06	r61	1.0944	a11102	99.23
r61	1.0969	a11102	111.18	r72	1.0946	a943	99.26	r72	1.0827	a943	99.48
r72	1.0933	a943	101.56	r82	1.0977	a51110	92.92	r82	1.0831	a51110	98.40
r82	1.0932	d111021	-75.73	r102	1.4226	d111021	47.36	r102	2.1554	d9431	121.50
r102	1.4593	d9431	272.07	r43	1.4519	d9431	223.81	r43	1.4673	d111021	-2.09
r43	1.4515	d4312	83.99	r94	0.9722	d4312	198.65	r94	0.9713	d4312	142.18
r94	0.9735	d6128	-66.54	r1110	1.4274	d511102	323.72	r1110	1.2730	d511102	0.18
r1110	1.3255	d82110	115.52	r511	1.2521	d72110	243.75	r511	1.2719	d72110	-96.23
a721	111.53	d72110	-120.54	a721	114.79	d82110	119.02	a721	120.58	d82110	97.14
a821	111.08	d31210	-66.08	a821	109.21	d31210	209.34	a821	120.52	d31210	-108.46
a1021	111.46	d51210	57.93	a1021	102.68	d61210	75.86	a1021	97.48	d61210	108.86
a431	107.72			a431	108.36			a431	107.11		



TS3											
parameter ^d	value	parameter ^d	value	parameter ^d	value	parameter ^d	value	parameter ^d	value	parameter ^d	value
r21	1.5142	r82	1.3317	a721	118.03	a612	109.39	d9431	-96.60	d61210	-73.53
r31	1.4121	r102	1.3890	a1021	116.33	a11102	88.92	d111021	-109.00	d51210	-192.47
r51	1.0981	r1110	1.5090	a431	107.44	a943	99.70	d4312	66.90	d31210	41.58
r61	1.0999	r43	1.4543	a312	113.50	a8210	85.70	d72110	141.99	d821011	2.08
r72	1.0954	r94	0.9762	a512	109.72						

^a Parameters: “R” corresponds to atomic distance between respective atoms in Angstroms, “A” parameter is the bond angle in degrees and “D” is the dihedral angle in degrees.

TABLE 2: Vibrational Frequencies (cm⁻¹) for Species in Ethyl Oxidation System Calculated at B3LYP/6-31G(d,p) Level of Theory^a

species	frequencies (cm ⁻¹)									moment of inertia (GHz)
•CH ₂ CH ₂ OOH (1a)	132.5 1067 3161	163 1141 3272	221 1274 3745	359 1365	461 1379	559 1459	842 1477	872 2987	966 3070	16.08 5.75 4.87
HOOCH ₂ CH(=O) (1b)	76 1075 3041	143 1109 3093	170 1253 3777	298 1339	420 1397	572 1412	729 1444	898 1843	1038 2911	13.67 2.94 2.63
H ₂ C=CHOOH (1c)	167 1159	243 1326	325 1385	620 1432	713 1728	849 3190	898 3206	974 3297	976 3742	18.54 6.6 4.95
HOOCH ₂ CH ₂ OO• (1d)	80 867 1394	110 922 1401	158 1008 1460	277 1062 1475	332 1127 3053	420 1171 3079	489 1281 3116	559 1296 3148	821 1377 3722	5.9 2.63 2.11
TS1 (1e)	1944(<i>i</i>) 852 1316	84 906 1387	103 935 1411	166 990 1499	247 1032 1776	355 1143 3036	432 1178 3110	572 1211 3127	666 1247 3760	9.83 1.8 1.64
TS2 (1f)	1106(<i>i</i>) 664 1361	88 809 1369	150 849 1409	183 926 1560	195 985 1609	367 1035 3091	378 1165 3194	484 1251 3294	522 1304 3762	5.83 2.25 1.75
TS3 (1g)	1821(<i>i</i>) 796 1349	111 830 1390	153 896 1425	208 904 1462	269 1033 1961	421 1089 3019	482 1109 3069	609 1147 3092	684 1276 3679	5.62 2.97 2.27

^a The frequencies reported are not scaled. Imaginary frequencies are denoted by "(*i*)." The alphanumeric below the species' names correspond to the species in Table 1.

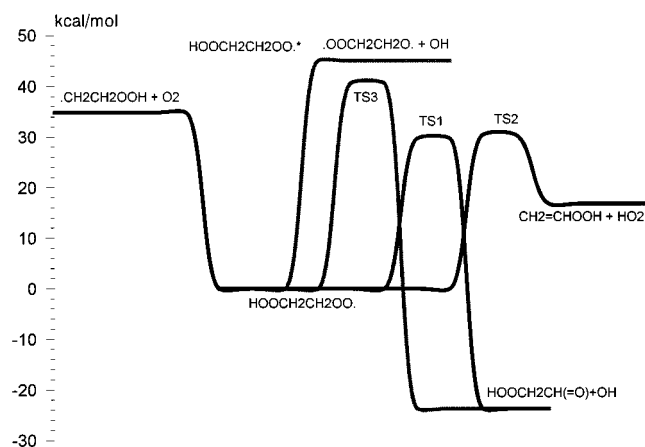


Figure 1. Potential energy diagram for the hydroperoxy-ethylperoxy oxidation system calculated at CBS-Q//B3LYP/6-31G(d,p).

Direct Molecular (HO₂) Elimination – TS2. The TS for the direct molecular elimination channel (denoted as TS2) has a breaking C–O bond length of 2.16 Å, and forming OO–H bond length of 1.27 Å and a breaking C–H bond length of 1.36 Å. The long C–O and OO–H bonds, the shorter O–O and C–C bonds, and near planar ethylene structure decisively determine this as the HO₂ molecular elimination TS.

Hydrogen Shift (Four-Member Ring) TS3. The third TS (denoted as TS3) is a four-member ring H-shift from the ipso-carbon to the peroxy oxygen. The C–H bond length in TS3 is 1.33 Å, and the O–H bond length is 1.27 Å. Again the C–O bond (1.39 Å) is shorter and the O–O bond (1.51 Å) is longer than normal, which infers the start of the OH elimination as in TS1. This transition state structure continues to react (eliminate OH) and form the strong carbonyl bond in hydroperoxy-acetaldehyde + OH. TS3 passes through a dihydroperoxy-ethyl radical structure, identical to TS1.

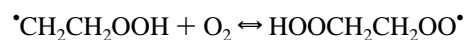
Diradical + OH Channel (HOOCH₂CH₂OO• ⇌ OH + •OCH₂CH₂OO•). The RO–OH bond energy in alkyl hydro-

peroxides is ca. 44.5 kcal/mol, which is only ca. 9 kcal/mol above the entrance channel of the hydroperoxy-ethyl + O₂. We include this channel in the chemical activation and dissociation reactions; because the molecule is relatively large and the bond cleavage has a loose transition state structure. Reints et al.¹⁰ report a generic Arrhenius A-factor for alkyl RO–OH dissociation of 3 × 10¹⁵ sec⁻¹, while Chen et al.²⁹ use 4.5 × 10¹⁵ sec⁻¹. We use this as an estimate, plus perform a sensitivity study showing results from increase and decrease of this A-factor by a factor of 3.3.

Thermodynamic Properties. The enthalpy of formation of the hydroperoxy-ethylperoxy radical, is calculated by isodesmic reaction analysis²¹ with B3LYP/6-31G(d,p) and CBS-Q//B3LYP/6-31G(d,p) ab initio calculations to be -24.01 and -23.89 kcal/mol, respectively. (Refer to Table 3) This is about 35 kcal/mol below the entrance channel and nearly identical to the well for ethyl radical + O₂. The thermodynamic properties of reactants, TS's and products of this system are listed in Table 4. TS1 and TS2 are very close in energy (within ca. 1 kcal/mol) and both are over 4 kcal/mol below the entrance channel. B3LYP/6-31G(d,p) and G3(MP2) calculate TS2 to be slightly lower in energy than TS1: but CBS-Q//B3LYP/6-31G(d,p) calculates TS1 slightly lower in energy than TS2, see Table 5. The 42.24 kcal/mol barrier of TS3 makes this channel unimportant.

Reaction Paths and High-Pressure Limit Rate Constants. The 2 hydroperoxy-ethyl radical undergoes addition with oxygen to form an energized 2-hydroperoxy-ethylperoxy radical, with no barrier and a 35.23 kcal/mol well depth at B3LYP/6-31G(d,p). CBS-Q//B3LYP/6-31G(d,p) determines this well depth to be 35.11 kcal/mol. The adduct (energized and stabilized) can undergo four possible reactions, with the high-pressure limit rate constants shown in Table 6. The reactions are as follows:

R(-11) Dissociation back to reactants



R12 five-member ring hydrogen shift forming an unstable dihydroperoxy-ethyl radical that rapidly β-scissions to hydro-

TABLE 3: Isodesmic Working Reactions for CBS-Q//B3LYP/6-31G(d,p) and B3LYP/6-31G(d,p) Analysis on Enthalpy of the Hydroperoxy–Ethylperoxy Adduct

CBS-Q//B3LYP/6-31G(d,p)						
HOOCH ₂ CH ₂ OOH –380.0054538 X X = –58.7 kcal/mol	+	C ₂ H ₆ –79.62475631 –20.4 ^a	=	CH ₃ CH ₂ OOH –229.8156475 –39.89 ^b	+	CH ₃ CH ₂ OOH –229.8156475 –39.89 ^b
HOOCH ₂ CH ₂ OO• –379.3699627 Y Y = –23.89 kcal/mol	+	CH ₃ CH ₂ OOH –229.8156475 –39.89 ^b	=	CH ₃ CH ₂ OO• –229.182771 –6.72 ^b	+	HOOCH ₂ CH ₂ OOH –380.0054538 –58.7
B3LYP/6-31G(d,p)						
HOOCH ₂ CH ₂ OOH –380.4196807 X X = –59.19 kcal/mol	+	C ₂ H ₆ –79.76083203 –20.4	=	CH ₃ CH ₂ OOH –230.0904115 –39.89 ^b	+	CH ₃ CH ₂ OOH –230.0904115 –39.89 ^b
HOOCH ₂ CH ₂ OO• –379.7921956 Y Y = –24.01 kcal/mol	+	CH ₃ CH ₂ OOH –230.0904115 –39.89 ^b	=	CH ₃ CH ₂ OO• –229.466121 –6.72 ^b	+	HOOCH ₂ CH ₂ OOH –380.4196807 –58.7

^a CRC Handbook of Chemistry and Physics, 63rd Ed., CRC Press, Inc. 1974 ^b On the basis of CBS-Q//B3LYP/6-31G(d,p) calculation with isodesmic working reactions. Refer to Sheng, C., Bozzelli, J. W., Dean, A. M., “Second Joint Meeting of the U. S. Sections of the Combustion Institute: Western States, Central States, Eastern States”, Oakland, CA, 2001

TABLE 4: Thermodynamic Properties of Species in the 2 Hydroperoxy–Ethylperoxy Oxidation System Calculated at CBS-Q//B3LYP/6-31G(d,p). Units: Enthalpy in kcal/mol, Entropy in cal/mol-K, Cp in cal/mol-K

species	H _f ^o ₂₉₈	S ^o ₂₉₈	Cp(300)	Cp(400)	Cp(500)	Cp(600)	Cp(800)	Cp(1000)	Cp(1500)
•CH ₂ CH ₂ OOH	11.22	83.28	20.25	23.52	26.36	28.72	32.30	35.13	39.67
O ₂	0	49.01	7.02	7.23	7.44	7.65	8.04	8.35	8.73
HOOCH ₂ CH ₂ OO•	–23.89	90.67	25.00	30.45	34.92	38.41	43.27	46.48	51.14
TS1	5.84	85.96	23.94	29.63	34.43	38.23	43.51	46.90	51.56
TS2	6.54	87.40	25.36	30.89	35.46	39.05	44.01	47.19	51.63
TS3	16.78	89.05	24.42	30.21	34.86	38.46	43.38	46.54	50.92
HOOCH ₂ CH(=O)	–57.06	83.24	21.07	25.20	28.66	31.42	35.31	37.90	41.61
H ₂ C=CHOOH	–10.87	73.59	17.67	21.58	24.80	27.33	30.83	33.16	36.61
HO ₂	3.25	54.73	8.37	8.95	9.48	9.96	10.78	11.43	12.47
OH	8.96	43.88	7.16	7.08	7.05	7.05	7.15	7.33	7.87

TABLE 5: Comparison of Activation Barriers, Relative to the Hydroperoxy–Ethylperoxy Adduct, for the Molecular Elimination and the five-member Ring Hydrogen Shift Transition State; CBS-Q//B3LYP/6-31G(d,p), B3LYP/6-31G(d,p) and G3(MP2)^a

	TS1 (five-member ring HS)	TS2 (molecular elimination)
B3LYP/6-31G(d,p)	29.05	28.25
CBS-Q//B3LYP/6-31G(d,p)	29.72	30.43
G3(MP2)	31.19	29.08
G3(MP2) (using B3LYP/6-31G(d,p) calculated ZPVE and thermal correction)	31.26	31.27

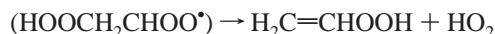
^a Units: kcal/mol.

peroxy-acetaldehyde plus OH. (TS1)



The typical O–O bond energy in a hydroperoxide ~45 kcal/mol, which is lower than the ~80 kcal/mol gained in the new π -bond of the C=O moiety. This reaction, over the H shift transition state, has some 54 kcal/mol excess energy over the product set HOOCH₂CH(=O) + OH. A significant fraction of the HOOCH₂CH(=O) has sufficient energy to cleave the RO–OH bond (45 kcal/mol) resulting in a second OH + a formyl methoxy radical (CH(=O)CH₃O•). This is a one new chain branching step; with the last step a function of both pressure and temperature.

R13 Molecular elimination, through a five-member ring, to form a hydroperoxy-ethylene molecule (H₂C=CHOOH) plus HO₂. (TS2)



R14 four-member ring hydrogen transfer on the ipso carbon forming an unstable dihydroperoxy-ethyl radical that rapidly β -scissions to hydroperoxy-acetaldehyde plus OH. (TS3) This HOOCH₂CH(=O) is also chemically activated; but with more energy, than **R12**.

R15 Cleavage of the weak hydroperoxide O–O bond in the energized [HO–OCH₂CH₂OO•]* adduct to form a diradical + OH



The two isomerization channels, **R12** and **R14**, both react to a dihydroperoxy-ethyl radical, which is unstable; it undergoes rapid β -scission, with no barrier, cleaving the weak RC•O–OH bond and forming a strong carbonyl bond, resulting in 2-hydroperoxy-acetaldehyde plus OH radical. (Figure 1). **R14** is not important because of its' higher barrier.

General Kinetic Implications. There are two low energy channels (**R12** and **R13**); both have similar rate constants and both result in low energy chain branching from chemical activation reactions of hydroperoxy alkyl radical associations

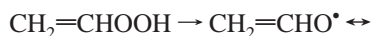
TABLE 6: High-pressure Limit Rate Constants. Rate Constants Expressed as $k_{\text{Forw}} = A T^n \exp(-E_a/RT)$ (units: cc/mol-s or s^{-1})

reaction (#)	A	n	E_a (kcal/mol)	comment
$\cdot\text{CH}_2\text{CH}_2\text{OOH} + \text{O}_2 \rightarrow \text{HOCH}_2\text{CH}_2\text{OO}\cdot$ (11)	2.94×10^{13}	-0.44	0.0	a
$\text{HOCH}_2\text{CH}_2\text{OO}\cdot \rightarrow \cdot\text{CH}_2\text{CH}_2\text{OOH} + \text{O}_2$ (-11)	8.20×10^{22}	-2.45	35.08	b
$\text{HOCH}_2\text{CH}_2\text{OO}\cdot \rightarrow \text{HOCH}_2\text{CH}(\text{=O}) + \text{OH}$ (HS) (12)	1.61×10^2	3.27	27.71	c
$\text{HOCH}_2\text{CH}_2\text{OO}\cdot \rightarrow \text{H}_2\text{C}=\text{CHOOH} + \text{HO}_2$ (ME) (13)	8.63×10^1	3.51	28.46	c
$\text{HOCH}_2\text{CH}_2\text{OO}\cdot \rightarrow \text{HOCH}_2\text{CH}(\text{=O}) + \text{OH}$ (ipso) (14)	1.75×10^3	3.19	38.90	c
$\text{HOCH}_2\text{CH}_2\text{OO}\cdot \rightarrow \cdot\text{OCH}_2\text{CH}_2\text{OO}\cdot + \text{OH}$ (15)	3.0×10^{15}	0.0	43.5	d

^a Used the rate constant from ethyl + $\text{O}_2 \rightarrow \text{CH}_3\text{CH}_2\text{OO}\cdot$ ^b Rate constant determine by satisfying the detailed balance criteria with current thermodynamic data ^c Rate constants calculated by canonical transition state theory. "HS" denotes through TS1, "ME" denotes through TS2 and "ipso" denotes through TS3. ^d Estimated preexponential A-factor from Reints et al. E_a is estimated by ΔH_{rxn} between products and reactants.

with O_2 and from thermal activation reactions of the stabilized peroxy adduct.

The hydroperoxy-ethylene from HO_2 elimination (R13) results in an important new chain branching channel, where the E_a reaction is ~ 22.5 kcal/mol. This is one-half the value of conventional chain branching activation energies. The vinyl hydroperoxide undergoes rapid unimolecular dissociation, breaking the weak O–O bond to form an OH plus vinyloxy radical^{22–24}



The vinyl hydroperoxide is probably formed with sufficient energy in moderate temperature combustion reactions to dissociate immediately; and even at thermal conditions it only has a short (several seconds) lifetime. This is a new, low energy, chain branching reaction and we look to learn and understand the implications of including this reaction in low to moderate temperature hydrocarbon and oxy-hydrocarbon oxidation systems and in oxidation of lubricating oils. We note a lower energy resonance structure of the vinyloxy radical is the formyl-methyl radical; it will further react with O_2 or undergo unimolecular isomerization/dissociation reactions.

The $\text{HOCH}_2\text{CH}(\text{=O})$ formed from R12 is chemically activated. It can dissociate before stabilization, or the stabilized molecule can undergo dissociation of the hydroperoxide bond to $\text{R}(\text{O}\cdot)\text{CH}(\text{=O}) + \text{OH}$, which is the conventional chain branching path, $E_a \approx 44$ kcal/mol (R3). The alkoxy-acetaldehyde radical can β -scission to either a di-aldehyde (glyoxal) + H atom or to a formyl radical plus formaldehyde. R3 has been considered important in recently published mechanisms, where the barrier was reduced to 37 kcal/mol for a better mechanism fit to data.^{25,26} The estimation of the preexponential A-factor for the cleavage of the O–O bond from $\text{ROOH} \rightarrow \text{RO}\cdot + \text{OH}$ is $4.5 \times 10^{15} \text{ s}^{-1}$.^{27,28}

It is surprising to find the barrier for the hydrogen shift to the peroxy radical from the β -carbon to be low, 29.72 kcal/mol, and similar to the HO_2 elimination barrier, 30.43 kcal/mol. This hydrogen transfer barrier is significantly lower than the isomerization barrier of ethyl-peroxy to hydroperoxy-ethyl, i.e., 36.36 kcal/mol.^{9,30,31} The reason for this low barrier is the very weak C–H bond energy on the hydroperoxide carbon, where the TST appears to recognize the lower energy, final products.¹⁹ The hydrogen transfer path (TS1) continues to lower energy products, and it also moves the hydroperoxy-ethyl radical out of the ethyl + O_2 quasi-equilibrium system; which serves to accelerate oxidation.

Kinetic Analysis on Chemical Activation $\text{C}\cdot\text{COOH} + \text{O}_2$ Reaction System. Rate constants calculated by QRRK analysis for $k(E)$ with master equation for falloff over a temperature range of 250–2500 K and a pressure range of 0.001–100 atm are performed. Nitrogen is used as the collision bath gas with a

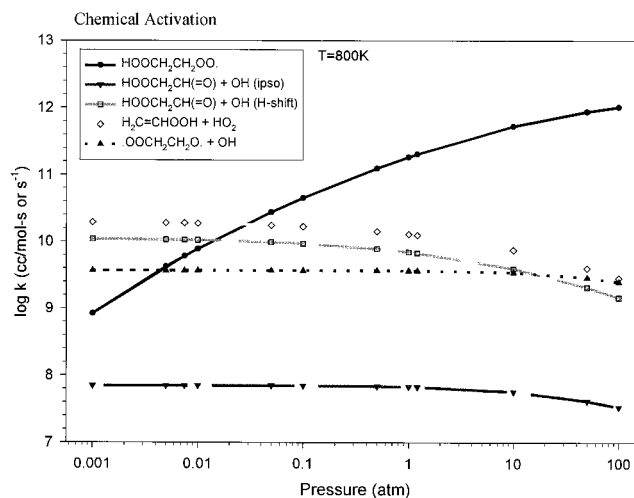


Figure 2. Rate Constants vs Pressure at $T = 800$ K.

ΔE_{down} of 830 cal/mol. The CBS-Q//B3LYP/6-31G(d,p) parameters are shown in Figure 2 for log rate constant versus log pressure at 800 K. This constant temperature analysis shows that stabilization is still increasing as pressure approaches 100 atm. The overriding reaction channels of the chemically activated adduct are stabilization at low T and high pressure, and dissociation of the adduct back to reactants. The molecular elimination to vinyl-hydroperoxide plus HO_2 , is the dominant product channel, but only factor of 1.8 faster than the low energy H-shift reaction and, surprisingly, only a factor of 3.5 faster than the higher energy chemical activation chain branching di-radical + OH product set at 1 atm. The formation rate of hydroperoxy-acetaldehyde plus OH, via the four-member ring ipso-carbon H-shift is slower than the five-member ring H-shift by over 2 orders of magnitude and is not important at lower temperatures. The five-member ring hydrogen shift and the molecular elimination channel are faster than the stabilization rate below 0.01 atm in the chemical activation reaction.

The dissociation kinetics of the chemically activated $\text{HOCH}_2\text{CH}(\text{=O})$ adduct from the H shift reactions will be treated in a future study.

A plot of rate vs temperature at 1.0 atm in Figure 3, shows complex temperature dependence. The stabilization rate constant for the hydroperoxy-ethylperoxy adduct is more important than product formation below 1000 K. The molecular elimination and the five-member ring H-shift channels are the most dominant products up to 800 K. The biradical + OH channel increases in importance with increase in temperature, and is near equal the HO_2 elimination channel at 1000 K. It is the most important product at higher T . Formation of hydroperoxy-acetaldehyde plus OH, via the four-member ring ipso-carbon H-shift is the least important channel.

Kinetic Analysis on Thermal Dissociation of $\text{HOCH}_2\text{CH}_2\text{OO}\cdot$ Adduct. It is important to analyze the adduct

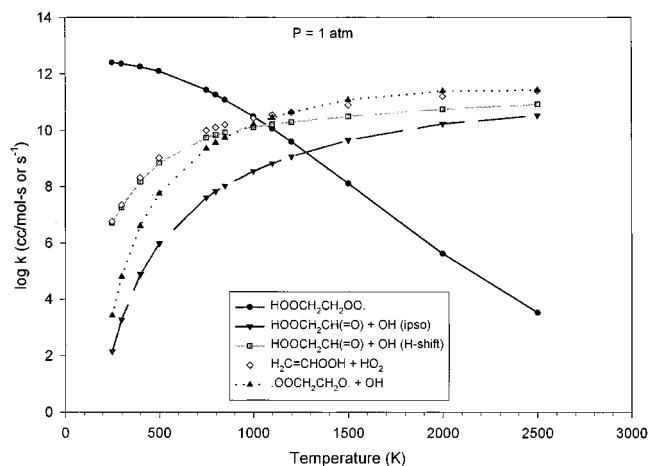


Figure 3. QRRK Rate Constants at $P = 1.0$ atm.

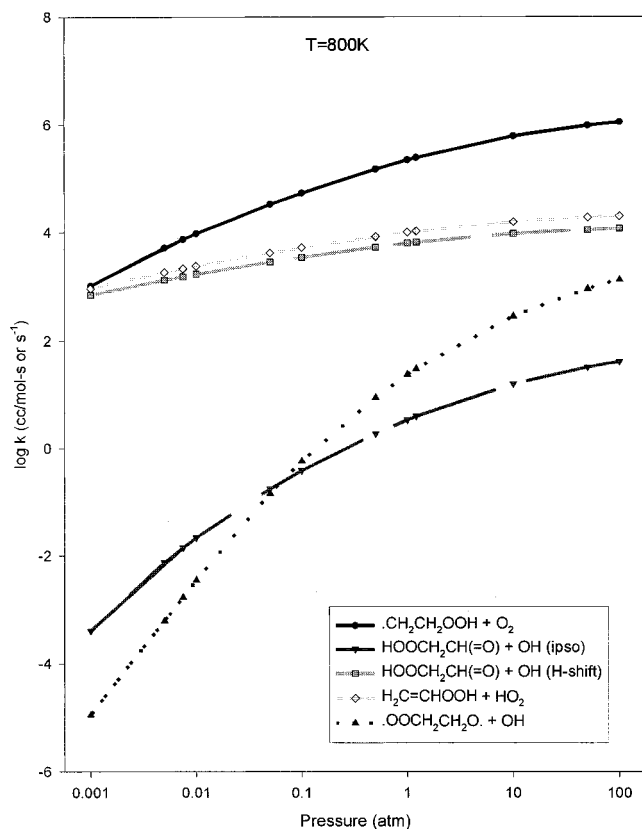


Figure 4. Dissociation rate constants for hydroperoxide ethyl peroxy radical calculated by QRRK with master equation analysis at isothermal conditions of $T = 800$ K.

dissociation due to the importance of stabilization. Dissociation rate constants at 800 K over a pressure range of 10^{-3} to 100 atm are illustrated in Figure 4. Dissociation to hydroperoxy-ethyl radical + O_2 is the most important channel, with HO_2 elimination and the H-shift isomerization channels showing a slight increase in rate constant with pressure. Dissociation of the stabilized adduct to the biradical + OH is increasing in importance with pressure.

Figure 5a and 5b illustrates dissociation rates at constant pressures of 0.0075 and 1.21 atm vs temperature. At 0.0075 atm pressure dissociation to hydroperoxy-ethyl radical + O_2 and the two similar barrier channels, HO_2 elimination and the H-shift isomerization, are all of similar importance. Above 1000 K, the two product channels dominate. As pressure is increased

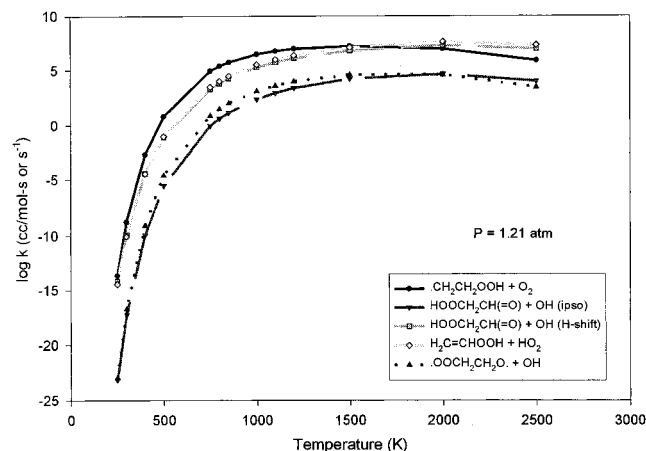
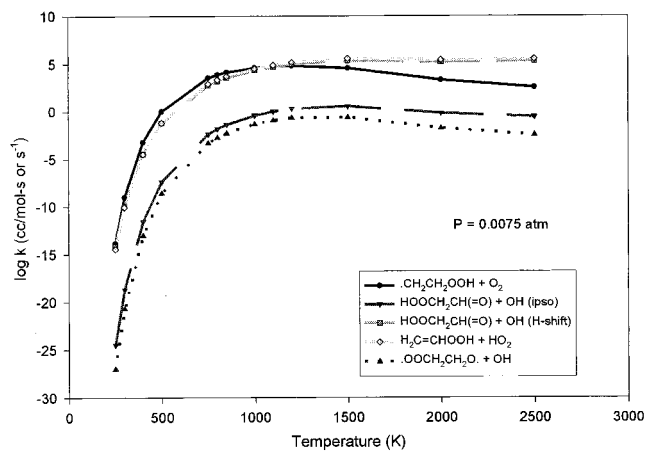
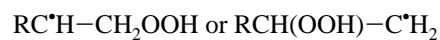


Figure 5. Thermal Dissociation rate constants for hydroperoxide ethyl peroxy radical calculated by QRRK with master equation analysis at isobaric conditions. Top 0.0075 atm, bottom = 1.21 atm..

to 1.21 atm, the reverse reaction to hydroperoxy-ethyl radical + O_2 is the dominant channel below 1500 K.

Sensitivity to R15. Figure 6 illustrates the sensitivity of R15 relative to the HO_2 elimination channel vs temperature when the Arrhenius A-factor is varied by \pm factor of 3.3 in the chemical activation system at low pressure. The HO_2 elimination and H-shift dominate below 1000 K but the importance of this diradical increases with temperature and pressure.

Formation of Hydroperoxy - Alkyl Radicals. If these newly proposed reactions are to be important in combustion and thermal oxidation systems; the paths for formation of the hydroperoxy-alkyl radical reactants need to occur. These are formed via two general mechanisms in combustion and other thermal oxidation systems. One via isomerization (H-shift) of peroxy radicals, particularly on hydrocarbons where 6 and seven-member H-shift ring transition states can occur. These larger rings have lower ring strain and thus lower barriers to the H-shift reactions. The second path is HO_2 radical addition to olefins²⁹



Summary

Thermochemical and kinetic parameters on the 2 hydroperoxy-ethyl radical reaction with molecular oxygen are determined for the first time. The standard enthalpy of formation for the hydroperoxide-ethylperoxy adduct is -23.89 kcal/mol and the reaction well depth is 35. kcal/mol. The activation barrier for the molecular elimination channel and the five-member ring

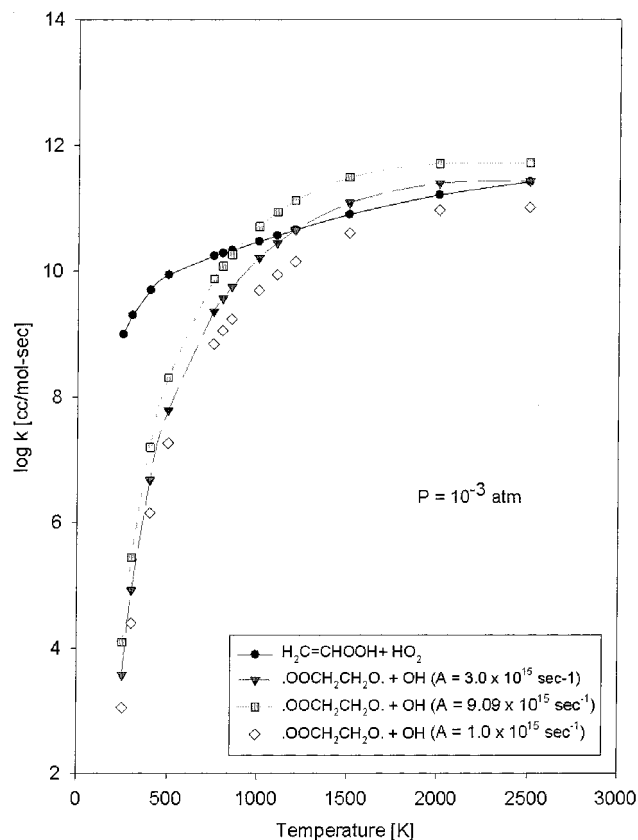


Figure 6. Sensitivity analysis of $\cdot\text{OCH}_2\text{CH}_2\text{OO}\cdot + \text{OH}$ channel. The molecular elimination channel is used as the reference comparison to the di-peroxy system.

hydrogen shift channels are calculated by CBS-Q//B3LYP/6-31G(d,p) {G3(MP2)} to be 30.43 {29.08} and 29.72 {31.19} kcal/mol. These barriers are 4 to 6 kcal/mol below the energy of the reverse reaction. The low barrier for the five-member ring isomerization reaction, some 7 kcal/mol lower than in the ethyl-peroxy system, is a result of the low C–H bond energies on the carbon bonding to the peroxide.

Chemical activation analysis on the reaction system shows prompt formation of the following: (i) a HO_2 molecular elimination plus vinyl-hydroperoxide, where the vinyl hydroperoxide has a weak (22 kcal/mol) $\text{CH}_2=\text{CHO}-\text{OH}$ bond and rapidly undergoes unimolecular dissociation to formyl methyl plus OH radicals; (ii) an intramolecular hydrogen transfer (five-member ring) to 2 hydroperoxide acetdehyde + OH, where the $\text{HOCH}_2\text{CH}(\text{=O})$ formed is chemically activated and a significant fraction dissociates to OH + formyl-methoxy radical, before stabilization; and (iii) a third new reaction path—cleavage of the weak peroxide bond to form a bi-radical + OH. The bi-radical + OH formation (**R15**) may have more importance in larger hydrocarbon radical systems, where the H-shift isomerizations to form hydroperoxide alkyl radicals have 6 and seven-member rings with low energy barriers. These larger molecules are also closer to the high-pressure limit.

Thermal dissociation of the stabilized adduct shows that the reverse reaction back to reactants is the dominant reaction below 1500 K at 1 atm; but HO_2 elimination and five-member ring H-shift (**R12** and **R13**), become competitive under lower pressure and temperature conditions.

The intramolecular H-transfer and HO_2 elimination reactions, **R12** and **R13**, have similar barriers and rate constants; they are important reactions in both chemical activation and in unimolecular dissociation; they move the hydroperoxy-ethyl radical

out of the ethyl + O_2 quasi-equilibrium and both lead to chain branching. Pressure effects on the rate constants of **R12** and **R13** are relatively small.

The overall (major flux) reaction paths are stabilization and reverse reaction to hydroperoxy-ethyl + O_2 . This forward/reverse reaction process results in a quasi-equilibria and allows the slower chain branching reaction steps, to exhibit a strong, and perhaps controlling influence under some conditions in hydrocarbon oxidation. We look to detailed mechanism studies with these reactions to amplify their significance in chain branching.

Acknowledgment. We acknowledge funding from the US EPA Airborne Organics Research Center. J.W.B. acknowledges technical interactions with Dr Anthony M. Dean on reactions of chemically activated species. We also acknowledge preprints to publication references 30 and 31 by the H. F. Schaefer III research group.

References and Notes

- (1) Walker, R. W.; Morley, C. *Basic Chemistry of Combustion*. In *Low-Temperature Combustion and Autoignition*; Pilling, M. J., Ed.; Elsevier: Amsterdam; New York, 1997; pp 1–124.
- (2) Ochteriski, J. W.; Petersson, G. A.; Montgomery, J. A. *J. Chem. Phys.* **1996**, *104*, 2598.
- (3) Curtiss, L. A.; Redfern, P. C.; Raghavachari, K.; Rassolov, V.; Pople, J. A. *J. Chem. Phys.* **1999**, *110*, 4703.
- (4) Frisch, M. J.; Trucks, G. W.; Head-Gordon, M.; Gill, P. M. W.; Wong, M. W.; Foresman, J. B.; Johnson, B. G.; Schlegel, H. B.; Robb, M. A.; Replogle, E. S.; Gomperts, R.; Andres, J. L.; Raghavachari, K.; Binkley, J. S.; Gonzalez, C.; Martin, R. L.; Fox, D. J.; Defrees, D. J.; Baker, J.; Stewart, J. J. P.; Pople, J. A.; Eds.; *Gaussian 94* computer program, Revision C.2; Gaussian Inc.: Pittsburgh, 1995.
- (5) Becke, A. D. *J. Chem. Phys.* **1993**, *98*, 5648.
- (6) Lee, C.; Yang, W.; Parr, R. G. *Phys. Rev. B* **1988**, *37*, 785.
- (7) Scott, A. P.; Radom, L. *J. Phys. Chem.* **1996**, *100*, 16 502–16 513.
- (8) Pitzer, K. S.; Gwinn, W. D. *J. Chem. Phys.* **1942**, *10*, 428.
- (9) Sheng, C.; Bozzelli, J. W.; Dean, A. M. "Thermochemical Parameters, Reaction paths and a Detailed Kinetic Model for the $\text{C}_2\text{H}_5 + \text{O}_2$ Reaction System"; Second Joint Meeting of the U. S. Sections of the Combustion Institute: Western States, Central States, Eastern States, 2001, Oakland, CA.
- (10) Reints, W.; Pratt, D. A.; Korth, H.-G.; Mulder, P. *J. Phys. Chem. A* **2000**, *104*, 10 713–10 720.
- (11) Westmoreland, P. R.; Howard, J. B.; Longwell, J. P.; Dean, A. M. *AIChE Annual Meeting*, 1986.
- (12) Westmoreland, P. R. *Combust. Sci. and Technol.* **1992**, *82*, 1515.
- (13) Dean, A. M.; Westmoreland, P. R. *Int. J. Chem. Kinet.* **1987**, *19*, 207.
- (14) Chang, A. Y.; Bozzelli, J. W.; Dean, A. M. *Zeit. Phys. Ch.* **2000**, *1533–1568*.
- (15) Gilbert, R. G.; Smith, S. C. *Theory of Unimolecular and Recombination Reactions*; Blackwell Scientific Publications: Oxford, 1990.
- (16) Gilbert, R. G.; Smith, S. C.; Jordan, M. J. T.; UNIMOL program suite (calculation of falloff curves for unimolecular and recombination reactions) Sydney, Australia, 1993.
- (17) Gilbert, R. G.; Luther, K.; Troe, J. *Ber. Bunsen-Ges. Phys. Chem.* **1983**, *87*, 164.
- (18) Zhong, X.; Bozzelli, J. W. *J. Phys. Chem. A* **1998**, *102*, 3537.
- (19) Bozzelli, J. W.; Jung, D. *J. Phys. Chem. A* **2001**, *105*, 3941–3946.
- (20) Stull, D. R.; Westrum, J., E. F.; Sinke, G. C. *The Chemical Thermodynamics of Organic Compounds*; Robert E. Krieger Publishing Company: Malabar, FL, 1987.
- (21) Hehre, W. J.; Radom, L.; Schleyer, P. R.; Pople, J. A. *Ab Initio Molecular Orbital Theory*; Wiley & Sons: New York, 1986.
- (22) Sebban, N.; Bockhorn, H.; Bozzelli, J. W. "Thermodynamic Properties and Reactions of Vinyl Hydroperoxides, Peroxy Radicals and Phenyl Hydroperoxide"; The Seventh International Congress on Toxic Combustion-byproducts: Origins, Fate and Health Effects, 2001, Research Triangle Park, NC.
- (23) Bach, R. D.; Ayala, P. Y.; Schlegel, H. B. *J. Am. Chem. Soc.* **1996**, *118*, 12 578–12 765.
- (24) Sebban, N.; Bockhorn, H.; Bozzelli, J. W. *Submitted to Phys. Chem. Chem. Phys.* **2001**.
- (25) Seiser, R.; Pitsch, H.; Seshadri, K.; Pitz, W. J.; Curran, H. J.

"Extinction and Autoignition of *n*-Heptane in Counterflow Configuration"; 28th International Symposium on Combustion, 2000, University of Edinburgh, Scotland.

(26) Ribaucour, M.; Minetti, R.; Sochet, L. R.; Curran, H. J.; Pitz, W. J.; Westbrook, C. K. "Ignition of Isomers of Pentane: An Experimental and Kinetic Modeling Study"; 28th International Symposium on Combustion, 2000, University of Edinburgh, Scotland.

(27) Chen, C.-J.; Bozzelli, J. W. *J. Phys. Chem. A* **2000**, *104*, 9715–9732.

(28) Mallard, W. G.; Westley, F.; Herron, J. T.; Hampson, R. F.; Frizzell, D. H.; NIST Chemical Kinetics Database; Version 2Q98 ed.; NIST Standard Reference Data: Gaithersburg, MD, 1998.

(29) Chen, C.-J.; Bozzelli, J. W. *J. Phys. Chem. A* **2000**, *104*, 4997–5012.

(30) Ignatyev, I. S.; Xie, Y.; Allen, W. D.; Schaefer III, H. F. *J. Chem. Phys.* **1997**, *107*, 141–155.

(31) Rienstra-Kiracofe, J. C.; Allen, W. D.; Schaefer III, H. F. *J. Phys. Chem. A* **2000**, *104*, 9823–9840.